ACS chemical biology

Articles

pubs.acs.org/acschemicalbiology

In Vivo Validation of Thymidylate Kinase (TMK) with a Rationally Designed, Selective Antibacterial Compound

Thomas A. Keating,*[,†] Joseph V. Newman,[†] Nelson B. Olivier,[‡] Linda G. Otterson,[†] Beth Andrews,[†] P. Ann Boriack-Sjodin,[†,‡] John N. Breen,[†,‡] Peter Doig,[†,‡] Jacques Dumas,[†] Eric Gangl,[†] Oluyinka M. Green,[†] Satenig Y. Guler,[†] Martin F. Hentemann,[†] Diane Joseph-McCarthy,[†] Sameer Kawatkar,[†] Amy Kutschke,[†] James T. Loch,[†] Andrew R. McKenzie,[†] Selvi Pradeepan,[†] Swati Prasad,[†] and Gabriel Martínez-Botella[†,§]

[†]AstraZeneca Infection Innovative Medicines, 35 Gatehouse Drive, Waltham, Massachusetts 02451, United States

[‡]AstraZeneca Discovery Sciences, 35 Gatehouse Drive, Waltham, Massachusetts 02451, United States

Supporting Information

ABSTRACT: There is an urgent need for new antibacterials that pinpoint novel targets and thereby avoid existing resistance mechanisms. We have created novel synthetic antibacterials through structure-based drug design that specifically target bacterial thymidylate kinase (TMK), a nucleotide kinase essential in the DNA synthesis pathway. A high-resolution structure shows compound TK-666 binding partly in the thymidine monophosphate substrate site, but also forming new induced-fit interactions that give picomolar affinity. TK-666 has potent, broad-spectrum Gram-positive microbiological activity (including activity against methicillin-resistant *Staphylococcus aureus* and vancomycin-resistant *Enterococcus*), bactericidal action with rapid killing kinetics, excellent target selectivity over the human ortholog, and low resistance rates. We demonstrate *in vivo* efficacy against *S. aureus* in a murine infected-thigh model. This work presents the first validation of TMK as a compelling antibacterial target and provides a rationale for pursuing novel clinical candidates for treating Gram-positive infections through TMK.

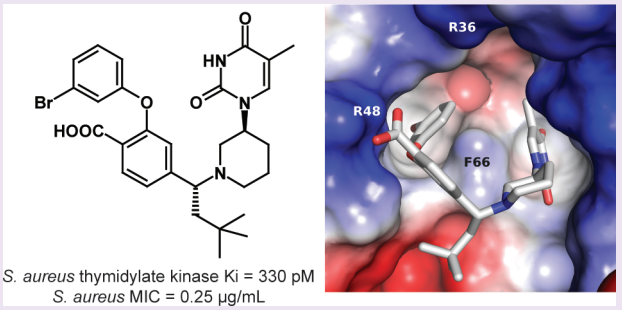

S. aureus thymidylate kinase Ki = 330 pM
S. aureus MIC = 0.25 μg/mL

Bacterial infections are a persistent and growing threat to human health due to emerging resistance to currently used antibiotics, but where new antibacterial development candidates will come from is an open question.[1] The early promise of an efficient and rational process to target identification, screening, and lead optimization has been judged a failure.[2] The field has returned to older methods, validating new antibacterial targets through natural products,[3] from whole-cell activity screens,[4] and from chemical genetics.[5] We remain committed to pioneering novel antibacterial targets through a bottom-up approach beginning with target selection.[6] We exploit the availability of complete genome sequences by analyzing bacterial gene products for conservation across pathogenic species (the potential for broad-spectrum activity) and divergence from human orthologs (the potential for selectivity). After target selection and evidence of genetic essentiality, structures are examined for suitable binding sites, and assay cascades are designed to efficiently prosecute the output of hit-finding methods such as activity or affinity screening or structure-based drug design. Optimized leads reveal key compound and target characteristics, such as spectrum and selectivity as well as bactericidality and resistance liability,[7] followed by preclinical target validation through *in vivo* efficacy.[6] We have created novel synthetic antibacterials through structure-based drug design that specifically target bacterial thymidylate kinase (TMK), a nucleotide kinase essential in the DNA synthesis pathway. Compound TK-666 has potent, broad-spectrum Gram-positive microbiological activity (including activity against methicillin-resistant *Staphylococcus aureus* and vancomycin-resistant *Enterococcus*), bactericidal action with rapid killing kinetics, excellent selectivity over the human ortholog, and low resistance rates. We demonstrate *in vivo* efficacy against *S. aureus* in a murine infected-thigh model. This work is the first that validates TMK as a compelling antibacterial target and demands pursuit of novel clinical candidates for treating Gram-positive infections through TMK.

TMK is an enzyme that transfers phosphate from ATP to thymidine monophosphate (dTMP) to form thymidine diphosphate (dTDP) and is an essential component of the thymidine triphosphate (dTTP) biosynthetic pathway. Disruption of TMK function is lethal to the cell because DNA replication is blocked.[8] Because TMK sits at the juncture of the *de novo* and salvage metabolic pathways leading to dTMP

Received: June 27, 2012
Accepted: August 21, 2012
Published: August 21, 2012

 © 2012 American Chemical Society

synthesis,[9] its inhibition negatively affects dTTP synthesis. TMK has been explored as an antimycobacterial[10] and antiviral[11] target, but despite effort,[12] compounds that validate TMK *in vivo* have not emerged because of the difficulty in converting lead inhibitors to development candidates.

RESULTS AND DISCUSSION

Examination of bacterial[13] and human TMK protein structures[14] suggested that the dTMP binding pocket was more amenable to structure-based rational drug design than the ATP site, because the dTMP site is less solvent-exposed and deeper and shares fewer conserved residues with human TMK (Supporting Figures 2–4). Previous work on TMK inhibitors[10,12] has shown that the thymine group helps retain potency and specificity. We designed as starting points simple analogues of the dTMP substrate, attaching to thymine a variety of heterocyclic rings as deoxyribose replacements, that were then further coupled to a second set of fragments of varying size and composition. We discovered TK-924 (Figure 1) by this targeted library approach as a suitable lead possessing

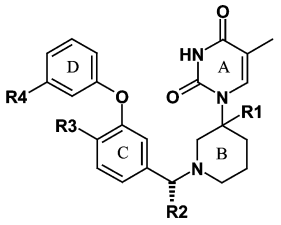

TK-924: **R1**=(*R*,*S*)-H; **R2**=H; **R3**=H; **R4**=H
TK-155: **R1**=(*S*)-H; **R2**=*n*-propyl; **R3**=COOH; **R4**=Cl
TK-666: **R1**=(*S*)-H; **R2**=*neo*-pentyl; **R3**=COOH; **R4**=Br

Figure 1. Chemical structure of TMK inhibitors TK-924 (racemic), TK-155, and TK-666 (absolute configurations). TK numbers are not sequential. The rings are lettered A–D for discussion.

weak but broad enzyme inhibition, and with some selectivity *versus* human TMK (Supporting Table 1). This racemic lead, however, is poorly soluble and hydrophobic and has little antibacterial activity. A dedicated medicinal chemistry program was started with goals to (i) improve potency for whole-cell activity with action through TMK, (ii) optimize physical properties for an intravenous delivery route and low toxicity potential, and (iii) achieve validation of TMK as an antibacterial target through *in vivo* efficacy. Over 1000 analogues were synthesized by a 10- to 15-step route and tested, supported by 59 crystal structures using the *Staphylococcus aureus* enzyme.[13] In an iterative design–make–test cycle motivated by structural analysis, several key improvements were made, beginning with resolution of (*S*)-TK-924 as the more potent enantiomer. Strikingly, this B-ring substitution pattern is the opposite of the dTMP substrate and was the first indication of a novel binding mode. Halogenating the D-ring to exploit a newly revealed hydrophobic pocket added both biochemical and antibacterial potency. Addition of the C-ring carboxylate dramatically improved solubility and further increased potency. Finally, addition of an alkyl group with appropriate stereochemistry between rings C and D contributed to structural stabilization and yielded TK-666 (Figure 1). As detailed below, TK-666 is a single enantiomer with excellent solubility, moderate clearance, broad-spectrum Gram-positive enzyme inhibition, rapid bactericidal activity, and efficacy in an *S. aureus* mouse model of infection. These features have allowed us to characterize TMK extensively as an antibacterial target.

Biochemical and Structural Characterization of a Potent, Selective Inhibitor. Biochemical inhibition (K_i) of the activity of *Streptococcus pneumoniae* and *S. aureus* TMK by TK-666 is extraordinarily potent (Table 1). TK-666 is also very

Table 1. Microbiological and Physiochemical Profile of TK-666[a]

enzyme	K_i (nM)
Staphylococcus aureus TMK	0.33
Streptococcus pneumoniae TMK	0.05
Escherichia coli TMK	17300
human TMK	17600
organism	**MIC (μg/mL)**
S. aureus (MSQS)	0.25
S. aureus (MIC_{90}, n = 22)	1
S. pneumoniae (Pen^R Ery^R)	0.016
S. pneumoniae (MIC_{90}, n = 19)	0.03
Streptococcus pyogenes	0.13
S. pyogenes (MIC_{90}, n = 21)	0.5
Streptococcus agalactiae	0.5
Staphylococcus epidermidis (MRSE)	2
Staphylococcus hemolyticus	0.06
Staphylococcus lugdunensis	0.03
Enterococcus faecium (LRE)	0.25
Enterococcus faecalis (VRE)	1
E. coli	>64
Haemophilus influenzae	>64
Pseudomonas aeruginosa	>64
Klebsiella pneumoniae	>64
Candida albicans	>64
human A549	>64
Sheep erythrocyte lysis	>64
TK-666 Properties	
molecular weight (g/mol)	584.5
equilibrium solubility pH 7.4 (μM)	750
Log D	1.09
plasma percent free (human/mouse)	3.2/<0.3
hepatocyte CLint (rat/mouse) (μL/min/1 × 10^6)	44/43

[a]MSQS = methicillin- and quinolone-sensitive. Pen^R Ery^R = penicillin- and erythomycin-resistant. MRSE = methicillin-resistant *S. epidermidis*. LRE = linezolid-resistant *Enterococcus*. VRE = vancomycin-resistant *Enterococcus*. MIC_{90} = minimal inhibitory concentration for 90% of n strains tested (MIC_{90}'s for levofloxacin in the panels were 16, 2, and 0.25 μg/mL for *S. aureus*, *S. pneumoniae*, and *S. pyogenes*, respectively). All other MICs are of single sentinel isolates.

selective, with human TMK inhibition 10^5- to 10^6-fold weaker. Gram-negative enzymes were not significantly inhibited by TK-666, as exemplified by a much weaker K_i against *Escherichia coli* TMK. We also evaluated the drug–drug interaction potential of TK-666 and found it selective *versus* the common cytochrome P_{450} enzymes (IC_{50} >20 μM against CYP1A2, 2C9, 2C19, 2D6, 3A4). We crystallized TK-666 bound to *S. aureus* TMK and obtained data suitable for refinement to 1.8 Å (Figure 2, Supporting Figure 1, Supporting Table 2). This structure shows TK-666 bound in the dTMP pocket and exemplifies the binding mode of the series. Thymine (A-ring) of the inhibitor is positioned similar to the natural substrate (Figure 2a,b) and interacts face-to-face with the phenyl ring of F66. Piperidyl ring B occupies the same region as the deoxyribose sugar of the

dx.doi.org/10.1021/cb300316n | *ACS Chem. Biol.* 2012, 7, 1866–1872

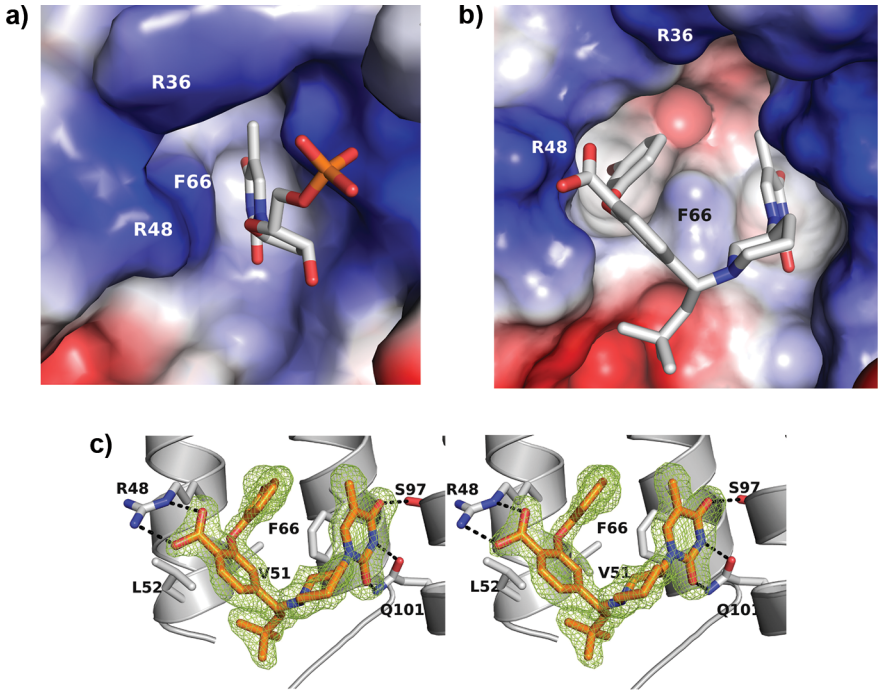

Figure 2. Crystal structure of TK-666 bound to *S. aureus* TMK and examination of induced fit. (a) *S. aureus* TMK with substrate dTMP.[13] Left of dTMP is the guanidinium group of R48, and R36 forms the upper region of the binding pocket. The ATP binding pocket is located out of the figure to the right. (b) TK-666 bound to *S. aureus* TMK in the dTMP site, solved at 1.8 Å (PDB ID 4GFD). Position of the thymine group is similar to the dTMP substrate, but the remainder of TK-666 points away from the substrate channel. Considerable space has been created by motions of R36 and R48 side chains, revealing a new hydrophobic pocket for ring D. (c) Stereo image highlighting polar interactions between TMK and TK-666. F66 is sandwiched by aromatic π-clouds of the inhibitor A- and D-rings. R36 and R48 now point away from the binding site as R48 forms a salt-bridge with the inhibitor carboxylate. The hydrophobic *neo*-pentyl substituent interacts with V51 and L52 side chains. The $F_o - F_c$ difference map (green mesh) was calculated in the absence of the inhibitor and contoured to 3σ.

substrate, but with a completely new orientation, pointing away from the dTMP-ATP substrate channel (Figure 2b). Strikingly, rings C and D now occupy a cryptic pocket not seen in the previously solved *S. aureus* TMK structures (Figure 2a), formed by the induced-fit binding of TK-666. This pocket is created by motions from R36 and R48 side chains and helix α2 to accommodate the inhibitor (Supporting Figure 1b). New, designed interactions are made between the carboxylate of ring C and the guanidinium of R48, ring D and the conserved REP-loop (residues 35−41), and the *neo*-pentyl substituent with the floor of the binding pocket toward conserved L52 and V51 (Supporting Figures 1−2). The D-ring also packs against the F66 phenyl on the face opposite of the A-ring. It is remarkable that despite the cryptic nature of this binding pocket, a high degree of conservation among the Gram-positive bacteria is retained (Supporting Figure 2, Table 1). A comparison with *E. coli*[15] and human[14] TMK structures (Supporting Figures 3 and 4) reveal differences in the binding regions of rings C and D that limit the bacterial spectrum of TK-666 to Gram-positives and confer selectivity over human TMK. In particular, the REP-loop and helix α2 of *E. coli* appear to intrude on the C/D-ring site. While the TK-924 lead has a fairly balanced K_i spectrum (Supporting Table 1), optimization for Gram-positive activity led to the divergence in *E. coli* binding potency seen for TK-666 (unpublished data). We expect that achievement of broad Gram-positive and Gram-negative activity with a single compound in this series may be unlikely.

Microbiological Spectrum and Mode of Action. TK-666 (Table 1) displays activity broadly against pathogenic Gram-positive bacteria while eukaryotic selectivity is seen *versus* fungus *Candida albicans*, human cell line A549, and red blood cells.[16] To assess activity against resistant strains, including methicillin-resistant *S. aureus* (MRSA) and penicillin-resistant *S. pneumoniae* (PRSP), data for small panels of 19−22 strains of *S. aureus*, *S. pneumoniae*, and *Streptococcus pyogenes* are reported as MIC_{90}'s (minimal inhibitory concentration for the 90th percentile of strains tested). Overall, there was no significant MIC difference against these resistant isolates, including linezolid- and vancomycin-resistant *Enterococcus*, relative to sensitive strains, demonstrating the potential of a novel antibacterial target and mechanism in combating drug-resistant bacteria. Characterization of the time-kill relationship[17] of TK-666 against *S. pneumoniae* and *S. aureus* is shown in Figure 3. A 0.5-, 1-, 2-, 4-, 8-, or 16-fold multiple of the MIC concentration of TK-666 was added to bacterial cultures, and remaining viable cells were counted at intervals. TK-666 showed rapid killing at 2-fold and greater the MIC against *S. pneumoniae* with slower killing at 0.5- and 1-fold MIC. Against *S. aureus*, the compound at 0.5-fold MIC and up showed concentration-dependent killing, *i.e.*, up to a three-log decrease in viable cell counts in 2 h. This bactericidal activity may offer a clinical advantage over bacteriostatic compounds in certain indications.[18]

Several lines of experimentation verified the microbiological mode of action of TK-666. The first was a radioactive metabolic precursor incorporation assay[19] in *S. aureus* that examined the effect of TK-666 on the synthesis of proteins, cell wall, fatty acids, RNA, and DNA. IC_{50}'s for the inhibition of the first three were >256 μg/mL. Only RNA and DNA syntheses were 50% inhibited at 10 and 0.3 μg/mL, respectively, consistent with the compound acting through inhibition of TMK. Second, the MIC

dx.doi.org/10.1021/cb300316n | *ACS Chem. Biol.* 2012, 7, 1866−1872

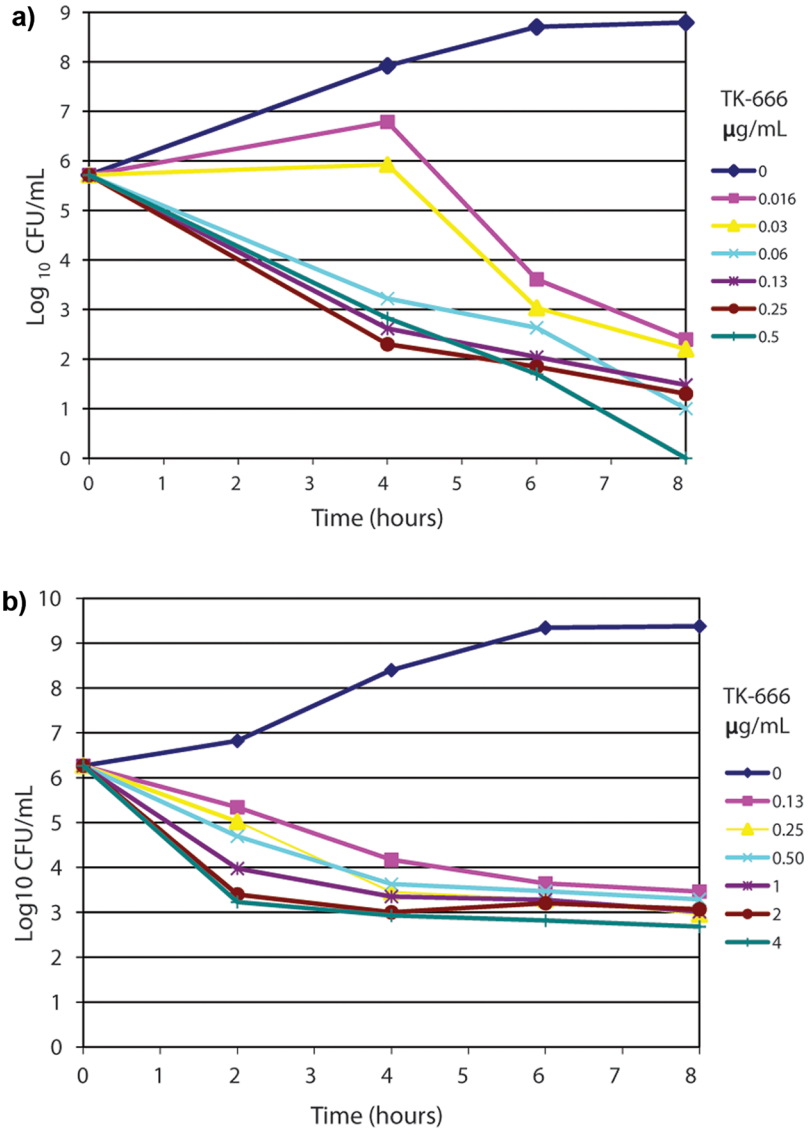

Figure 3. Characterization of bactericidality. (a) Time-kill rate of TK-666 against *S. pneumoniae*. TK-666 was added at 0.5-, 1-, 2-, 4-, 8-, or 16-fold of the predetermined MIC of 0.03 μg/mL to liquid cultures of *S. pneumoniae*. A negative control for uninhibited growth was included. Samples were removed at regular intervals, plated on nutrient agar, and incubated, and viable colony-forming units (CFU) were counted after growth. The limit of detection is 100 CFU/mL. Rapid killing of three logs in 4 h was observed at 2-fold MIC and above, indicating bactericidality. (b) Killing rate of TK-666 against *S. aureus*. Fold dilutions relative to the predetermined MIC of 0.25 μg/mL were as above. Rapid and TK-666 concentration-dependent killing of up to three logs in 2 h was observed, with bactericidality observed at concentrations of 0.5-fold MIC and above.

in *S. pneumoniae* of a TMK-overexpressing strain was elevated 8-fold as compared to the parent strain. Third, TK-666 showed cross-resistance against a *tmk* G44S mutant generated with analogue TK-155 at frequencies 2×10^{-9} and 5×10^{-9} at 4- and 8-fold the MIC (TK-series MICs were elevated 8- to 32-fold). This indicates that growth suppression in *S. aureus* by TK-666 is caused through inhibition of TMK. For *S. pneumoniae*, mutants against TK-666 could be isolated at 4- and 8-fold the MIC at frequencies of 3×10^{-9} and 5×10^{-10}, respectively, showing high (8- to >256-fold) MIC increases compared to the parent strain. Upon sequencing, base pair changes were found in *tmk* that resulted in an amino acid change at the binding site for TK-666: Y71 to Cys or His. Both the G44S and the Y71 mutants map to the inhibitor binding site in TMK (Supporting Figure 1b).

***In Vivo* Efficacy against *S. aureus*.** We demonstrated *in vivo* efficacy of TK-666 in a murine model of *S. aureus* thigh infection (Figure 4). Mice were infected in a single thigh with *S. aureus*, followed 2 h later by administration of a single intraperitoneal dose of TK-666 (30, 50, 100, or 200 mg/kg) or multiple doses of 200 mg/kg up to 800 mg/kg total (Figure 4a). Pharmacokinetic data were collected from blood samples over a period of 24 h from a satellite group of mice (Figure 4b). TK-666 was well-tolerated, with no observable adverse effects seen up to and including the highest dose. Colony counts in infected tissue 24 h after the start of treatment showed a 0.5-log drop at 100 mg/kg dose compared to the untreated control group, with stasis (defined as maintenance of inoculum burden) interpolated to 150 mg/kg. This compares favorably to the static dose for levofloxacin, 40 mg/kg. These results provide unambiguous *in vivo* validation for TMK as an antibacterial target. While these data are not designed to identify the PK/PD driver for efficacy, we observe that stasis is achieved at total blood exposures of 210 μg·h/mL (AUC) and 80 μg/mL (C_{max}).

dx.doi.org/10.1021/cb300316n | *ACS Chem. Biol.* 2012, 7, 1866–1872

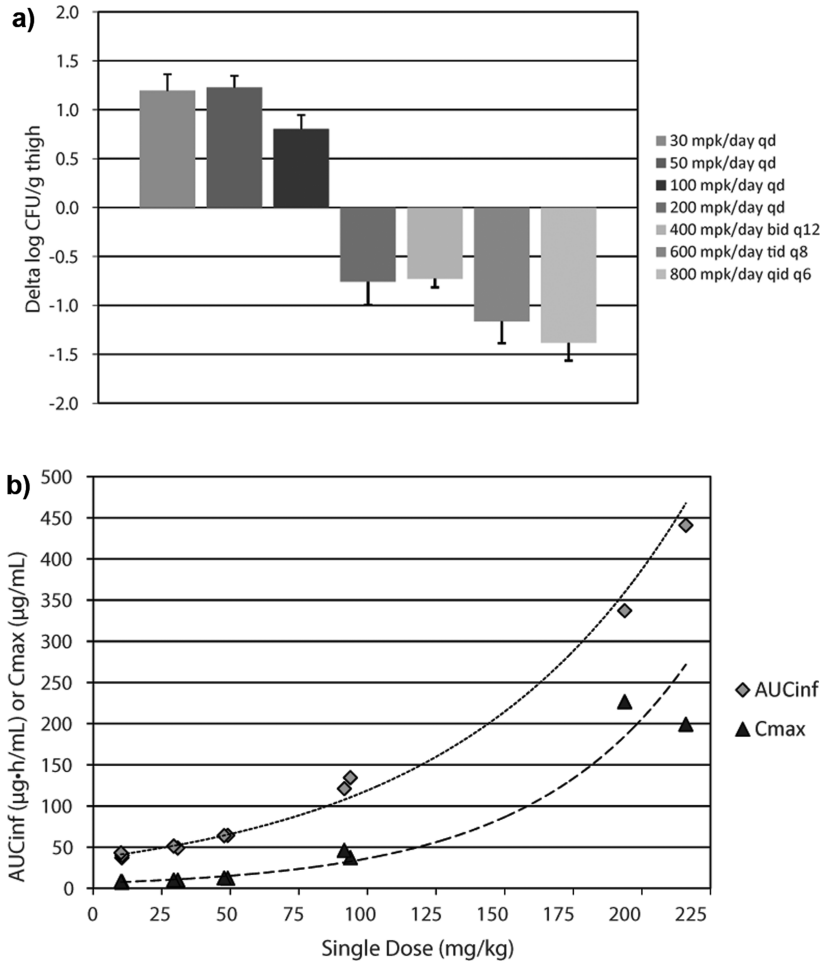

Figure 4. *In vivo* efficacy and pharmacokinetics of TK-666. (a) Dose−response results of TK-666 in a murine model of *S. aureus* thigh infection. Immunocompetent mice were infected in a single thigh with *S. aureus* followed 2 h later by intraperitoneal administration of TK-666 as single doses (qd) up to 200 mg/kg; or twice, every 12 h (bid q12); thrice, every 8 h (tid q8); or four times, every 6 h (qid q6) per day, up to 800 mpk/day. There were no observable adverse effects up to and including the highest dose. Efficacy was determined by harvesting infected tissue 24 h after the start of treatment. Vehicle yielded CFU counts equivalent to the lowest two doses (1.25-log growth), while doses at 100 mg/kg or higher were efficacious. Stasis, defined as no change in CFU from start of treatment, is achieved at ∼150 mg/kg single dose (interpolated). The corresponding static dose for levofloxacin in this model is 40 mg/kg. (b) Pharmacokinetics of TK-666 carried out in conjunction with efficacy experiments, measured in blood plasma taken from satellite groups of infected mice. Compound was administered in single doses as above. AUC_{inf} (integrated area under the curve with last concentration extrapolated) and C_{max} showed nonlinear increases in exposure with increased doses.

We propose that these relatively large doses required for TK-666 efficacy are due to the high degree of protein binding in mouse plasma (<0.3% free, Table 1), which results in free TK-666 concentrations in plasma at stasis of approximately 0.6 μg·h/mL (AUC) and 0.3 μg/mL (C_{max}). Translated to human dosing, the 10-fold higher free fraction in human plasma should allow these efficacious concentrations to be reached with lower doses.

Although novel antibacterial targets offer an opportunity to avoid the resistance and selectivity limitations of existing classes of drugs, only about a half dozen have successfully reached *in vivo* efficacy in the past decade,[3−6,20] and only twice beginning with target selection, including this work.[6] The difficulty is clear: following evidence of genetic essentiality of the target and evaluation of selectivity and spectrum potential, compounds must be found, through screening or design, that bind specifically to a druggable site. The potency and physical properties necessary for whole-cell activity must be developed and optimized, and acceptable safety and exposure must be maintained to achieve positive *in vivo* efficacy. A careful and rigorous approach to each step can not only yield development candidates but also lay a strong foundation for further, rational work. In TK-666, we have identified a novel class of antibacterials that selectively inhibits TMK and DNA synthesis in Gram-positive bacteria, and this work provides the rationale for developing a clinical candidate against this target to treat Gram-positive infections. The compound possesses a favorable MIC profile, killing kinetics, selectivity, barriers to resistance, physical properties, *in vivo* tolerability, and efficacy. The critical questions for clinical validation need to be addressed next: *in vivo* safety profile, human pharmacokinetics, and clinical resistance potential. This work demonstrates the power of modern target selection and structure-based drug discovery to validate and enable quality novel targets for therapeutic intervention and adds TMK to the limited list of such targets.

METHODS

Synthesis of TK-924, TK-666, and TK-155. Detailed experimental routes, analysis, and characterization are included in Supporting Information.

dx.doi.org/10.1021/cb300316n | *ACS Chem. Biol.* 2012, 7, 1866−1872

S. aureus Thymidylate Kinase K_i Assay. Activity was assayed in the reverse direction by measuring the conversion of dTDP to dTMP with concomitant conversion of ADP to ATP. Production of ATP was coupled to luciferin/luciferase, and the luminescence was calibrated to inhibition. The assay mixture consisted of 50 mM Hepes-NaOH pH 8.0, 0.005% Brij-35, 10 mM $MgCl_2$, 25 mM sodium acetate, 5 mM dithiothreitol (DTT), 0.5 mM EDTA, 200 μM ADP, 2000 μM dTDP, 1 nM *S. aureus* TMK.[13] Assays were conducted at room temperature (RT) in a 30 μL volume in 384-well plates (Costar no. 3572). For IC_{50} measurements, compounds were prepared as 10 mM stock solutions in dimethyl sulfoxide (DMSO), and 10-point, 2-fold, serial dilutions were prepared from these stocks using DMSO, 600 nL of which was added to the wells before assay buffer (final DMSO 2%). After 3.5 h, 15 μL of ATPlite detection reagent (PerkinElmer) was added, and the luminescence was read. Percent inhibition data were fit to the standard IC_{50} equation, and K_i's were calculated from the Cheng–Prusoff relationship for competitive inhibitors: $K_i = IC_{50}/(1 + ([S]/K_M))$ where [S] and K_M are the dTDP concentration and Michaelis constant, respectively. Methods for *S. pneumoniae*, *E. coli*, and human TMK K_i assays are included in Supporting Information.

Physical Properties. Methods for determination of log D, plasma protein binding, hepatocyte metabolism, and equilibrium solubility are included in Supporting Information.

Microbiology. Methods for MIC determination, time-kill, and mode-of-action assays are included in Supporting Information.

Crystal Structure of TK-666 Bound to _S. aureus_ TMK. To obtain the inhibitor-bound crystal form of *S. aureus* TMK, crystals were initially grown in the absence of compound using the sitting drop method at 20 °C with a reservoir solution of 100 mM PCPT (propionate-cacodylate-bis-tris propane buffer) pH 7–8, 21–24% PEG 3350, 200 mM $MgCl_2$ using a 1:1 protein/reservoir solution with the protein solution at 13 mg/mL. Crystals were harvested and soaked overnight in a solution containing 100 mM PCPT, 35% PEG-3350, 200 mM Mg_2Cl, and 1–2 mM TK-666 from a 100 mM DMSO stock. After soaking the crystals were cryoprotected by soaking for 15 min in compound-soak solution supplemented with 20% ethylene glycol. Cryoprotected crystals were mounted on nylon loops and flash-cooled in liquid nitrogen. Data were collected at the Advanced Photon Source of Argonne National Laboratory on the LRL-CAT beamline. Data reduction was accomplished by employing the autoproc toolbox, and the structure was determined by molecular replacement with AMoRE using an apo-state model of *S. aureus* TMK. COOT was used to inspect the model and electron density, and BUSTER was used for macromolecular refinement calculations. Geometry of the model was analyzed with MolProbity, and stereochemistry of the compound was analyzed with MOGUL. Crystallographic data collection and model refinement statistics are in Supporting Table 2. The structure has been deposited in the Protein Data Bank with accession code 4GFD.

Immunocompetent Murine Thigh _S. aureus_ Efficacy Model. All procedures were carried out according to a protocol approved by the Institutional Animal Care and Use Committee (IACUC). TK-666 was formulated as a 20 mg/mL solution in 0.2 M meglumine/10% 2-hydroxypropyl-β-cyclodextrin, pH 8. Two hours prior to infection, mice received a single administration of 100 mg/kg 1-amino-benzotriazole (ABT) orally to inhibit CYP_{450} activity.[21] This had the moderate effect of increasing exposure by 50% to 100% over untreated animals and was employed because of the moderate hepatocyte clearance observed in mice (43 μL/min/1 × 10^6). A late-log culture of *S. aureus* ARC516 was diluted to a concentration of ~1.4 × 10^7 CFU/mL. The bacterial density was determined by dilution and plating for viable counts. Mice, anesthetized with isofluorane, were infected with 70 μL of culture postlaterally, into the right thigh muscle, to achieve a target starting inoculum of 1 × 10^6 CFU/thigh. Mice were then assigned to control or treatment groups. Two hours after infection, one group of 10 mice was euthanized to determine the mean CFU in the infected thighs at start of treatment. The remaining groups of mice were administered (1) a single dose of TK666 of 30, 50, 100, or 200 mg/kg or multiple doses of 200 mg/kg equally spaced over 24 h to reach totals of 400, 600, or 800 mg/kg; (2) levofloxacin; or (3) vehicle. Mice were euthanized 24 h after start of treatment by carbon dioxide asphyxiation and cervical dislocation, and the infected thigh was removed and dissected. The thighs were weighed and transferred to tubes containing 1 mL of tryptic soy broth for homogenization. Thigh tissue was homogenized (Omni TH homogenizer, Omni International), and 100 μL of homogenate serially diluted in tryptic soy broth and plated onto tryptic soy agar plates for CFU determination. Plates were incubated at 37 °C overnight. Thigh tissue homogenates were bioanalyzed.

Satellite Pharmacokinetics. Groups of satellite mice infected with *S. aureus*, as described, were used for determining plasma concentrations. Dosing started 2 h after infection, and whole blood samples were taken at various time points. Whole blood was sampled into microcontainer tubes containing ethylenediamine tetraacetic acid (EDTA, Beckton Dickinson). Three mice per time point were used. Plasma was separated by centrifugation for 5 min at 13,200 rpm and stored at −80 °C until bioanalysis.

Bioanalysis. Bioanalysis was performed by LC–MS/MS using Shimadzu liquid chromatography, a LEAP Technologies CTC-PAL autosampler, and an Applied Biosystems API 4000 mass spectrometer. Plasma samples were protein-precipitated with acetonitrile/methanol (80:20) containing carbutamide as the internal standard (Sigma-Aldrich). LC was performed in gradient mode using a Phenomenex Gemini-NX 3 μm C18 column (part no. 00A-4453-Y0). The mobile phase A was 10 mM ammonium formate with 0.1% formic acid in water, and mobile phase B was 0.1% formic acid in acetonitrile. Gradients were run from 10% B to 90% B in ~2.5 min. Mass spectrometer detection was conducted in MRM mode using the following mass transitions: TK-666 (584.24/210.22) and carbutamide (272.10/156.10).

Pharmacokinetic Data Analysis. The plasma profile for each dose group was obtained by calculating the average plasma concentration of compound in each of the three animals per time point. The area under the plasma concentration time curve from zero to infinity with extrapolation of the last point (AUC_{inf}), maximum plasma drug concentration (C_{max}), time to reach maximum concentration (t_{max}), and plasma half-life ($t_{1/2}$) for each dose group was determined by non-compartmental analysis (WinNonLin 4.1, Pharsight). The non-compartmental Model 200 was used in the analysis.

The AUC values for the bid, tid, and qid dose regimens were determined by multiplying the AUC value obtained after a single dose by the number of doses administered, assuming linear pharmacokinetics and no accumulation after multiple doses. C_{max} for the fractionated doses was also determined under the assumption of linear pharmacokinetics.

■ ASSOCIATED CONTENT

Ⓢ Supporting Information

This material is available free of charge *via* the Internet at http://pubs.acs.org.

■ AUTHOR INFORMATION

Corresponding Author

*E-mail: thomas.keating@astrazeneca.com.

Present Address

§Sage Therapeutics, 215 First Street, Cambridge, MA 02141.

Notes

The authors declare no competing financial interest.

■ ACKNOWLEDGMENTS

We thank J. Macritchie, J. Duffy, and colleagues at BioFocus (Saffron Walden, U.K.) for collaborative work leading to TK-924 and M. Kannan and team at Syngene (Bangalore, India) for chemistry support. We thank AstraZeneca Infection colleagues S. Lahiri and T. Palmer for early work on TMK, N. DeGrace and N. Bezdenejnih-Snyder for analytical support, and R. Alm and M. Johnstone for resistance profiling/sequencing.

REFERENCES

(1) Fischbach, M. A., and Walsh, C. T. (2009) Antibiotics for emerging pathogens. *Science 325*, 1089−1093.

(2) Payne, D. J., Gwynn, M. N., Holmes, D. J., and Pompliano, D. L. (2007) Drugs for bad bugs: confronting the challenges of antibacterial discovery. *Nat. Rev. Drug Discovery 6*, 29−40.

(3) Wang, J., Soisson, S. M., Young, K., Shoop, W., Kodali, S., Galgoci, A., Painter, R., Parthasarathy, G., Tang, Y. S., Cummings, R., Ha, S., Dorso, K., Motyl, M., Jayasuriya, H., Ondeyka, J., Herath, K., Zhang, C., Hernandez, L., Allocco, A., Basilio, A., Tormo, J. R., Genilloud, O., Vicente, F., Palaez, F., Colwell, L., Lee, S. H., Michael, B., Felcetto, T., Gil, C., Silver, L. L., Hermes, J. D., Bartizal, K., Barrett, J., Schmatz, D., Becker, J. W., Cully, D., and Singh, S. B. (2006) Platensimycin is a selective FabF inhibitor with potent antibiotic properties. *Nature 441*, 358−360.

(4) Andries, K., Verhasselt, P., Guillemont, J., Goehlmann, H. W. H., Neefs, J.-M., Winkler, H., Gestel, J. V., Timmerman, P., Zhu, M., Lee, E., Williams, P., Chaffoy, D. d., Huitric, E., Hoffner, S., Cambau, E., Truffot-Pernot, C., Lounis, N., and Jarlier, V. (2005) A diarylquinoline drug active on the ATP synthase of *Mycobacterium tuberculosis*. *Science 307*, 223−227.

(5) Haydon, D. J., Stokes, N. R., Ure, R., Galbraith, G., Bennett, J. M., Brown, D. R., Baker, P. J., Barynin, V. V., Rice, D. W., Sedelnikova, S. E., Heal, J. R., Sheridan, J. M., Aiwale, S. T., Chauhan, P. K., Srivastava, A., Taneja, A., Collins, I., Errington, J., and Czaplewski, L. G. (2008) An inhibitor of FtsZ with potent and selective anti-staphylococcal activity. *Science 321*, 1673−1675.

(6) Mills, S. D., Eakin, A. E., Buurman, E. T., Newman, J. V., Gao, N., Huynh, H., Johnson, K. D., Lahiri, S., Shapiro, A. B., Walkup, G. K., Yang, W., and Stokes, S. S. (2011) Novel bacterial NAD^+-dependent DNA ligase inhibitors with broad-spectrum activity and antibacterial efficacy *in vivo*. *Antimicrob. Agents Chemother. 55*, 1088−1096.

(7) O'Neill, A. J., and Chopra, I. (2004) Preclinical evaluation of novel antibacterial agents by microbiological and molecular techniques. *Expert Opin. Investig. Drugs 13*, 1045−1063.

(8) Petit, C. M., and Koretke, K. K. (2002) Characterization of *Streptococcus pneumoniae* thymidylate kinase: steady-state kinetics of the forward reaction and isothermal titration calorimetry. *Biochem. J. 363*, 825−831.

(9) Zaritsky, A., Woldringh, C. L., Einav, M., and Alexeeva, S. (2006) Use of thymine limitation and thymine starvation to study bacterial physiology and cytology. *J. Bacteriol. 188*, 1667−1679.

(10) Vanheusden, V., Munier-Lehmann, H., Froeyen, M., Busson, R., Rozenski, J., Herdewijn, P., and Calenbergh, S. V. (2004) Discovery of bicyclic thymidine analogues as selective and high-affinity inhibitors of *Mycobacterium tuberculosis* thymidine monophosphate kinase. *J. Med. Chem. 47*, 6187−6194.

(11) Brundiers, R., Lavie, A., Veit, T., Reinstein, J., Schlichting, I., Ostermann, N., Goody, R. S., and Konrad, M. (1999) Modifying human thymidylate kinase to potentiate azidothymidine activation. *J. Biol. Chem. 274*, 35389−35292.

(12) Choi, J. Y., Plummer, M. S., Starr, J., Desbonnet, C. R., Soutter, H., Chang, J., Miller, J. R., Dillman, K., Miller, A. A., and Roush, W. R. (2012) Structure guided development of novel thymidine mimetics targeting *Pseudomonas aeruginosa* thymidylate kinase: from hit to lead generation. *J. Med. Chem. 55*, 852−870.

(13) Kotaka, M., Dhaliwal, B., Ren, J., Nichols, C. E., Angell, R., Lockyer, M., Hawkins, A. R., and Stammers, D. K. (2006) Structures of *S. aureus* thymidylate kinase reveal an atypical active site configuration and an intermediate conformational state upon substrate binding. *Protein Sci. 15*, 774−784.

(14) Ostermann, N., Schlichting, I., Brundiers, R., Konrad, M., Reinstein, J., Veit, T., Goody, R. S., and Lavie, A. (2000) Insights into the phosphoryltransfer mechanism of human thymidylate kinase gained from the crystal structures of enzyme complexes along the reaction coordinate. *Structure 8*, 629−642.

(15) Lavie, A., Ostermann, N., Brundiers, R., Goody, R. S., Reinstein, J., Konrad, M., and Schlichting, I. (1998) Structural basis for efficient phosphorylation of 3′-azidothymidine monophosphate by *Escherichia coli* thymidylate kinase. *Proc. Natl. Acad. Sci. U.S.A. 95*, 14045−14050.

(16) CLSI (2009) *Methods for Dilution Antimicrobial Susceptibility Tests for Bacteria That Grow Aerobically; Approved Standard-Eighth ed.*, document M07-A8, Clinical and Laboratory Standards Institute, Wayne, PA.

(17) CLSI (1999) *Methods for Determining Bactericidal Activity of Antimicrobial Agents; Approved Guideline*, document M26-A, Clinical and Laboratory Standards Institute, Wayne, PA.

(18) Pankey, G. A., and Sabath, L. D. (2004) Clinical relevance of bacteriostatic versus bactericidal mechanisms of action in the treatment of Gram-positive bacterial infections. *Clin. Infect. Dis. 38*, 864−870.

(19) Hilliard, J. J., Goldschmidt, R. M., Licata, L., Baum, E. Z., and Bush, K. (1999) Multiple mechanisms of action for inhibitors of histidine protein kinases from bacterial two-component systems. *Antimicrob. Agents Chemother. 43*, 1693−1697.

(20) Schneider, T., Kruse, T., Wimmer, R., Wiedemann, I., Sass, V., Pag, U., Jansen, A., Nielsen, A. K., Mygind, P. H., Raventós, D. S., Neve, S., Ravn, B., Bonvin, A. M. J. J., Maria, L. D., Andersen, A. S., Gammelgaard, L. K., Sahl, H.-G., and Kristensen, H.-H. (2010) Plectasin, a fungal defensin, targets the bacterial cell wall precursor lipid II. *Science 328*, 1168−1172.

(21) Balani, S. K., Li, P., Nguyen, J., Cardoza, K., Zeng, H., Mu, D.-X., Wu, J.-T., Gan, L.-S., and Lee, F. W. (2004) Effective dosing regimen of 1-aminobenzotriazole for inhibition of antipyrine clearance in guinea pigs and mice using serial sampling. *Drug Metab. Dispos. 32*, 1092−1095.